Dalton Transactions

Nitratoethyl-5H-tetrazoles: Improving Oxygen Balance through Application of Organic Nitrates in Energetic Coordination Compounds

Journal:	*Dalton Transactions*
Manuscript ID	DT-ART-06-2021-001898.R1
Article Type:	Paper
Date Submitted by the Author:	28-Jun-2021
Complete List of Authors:	Stierstorfer, Joerg; LMU, Chemistry Gruhne, Michael; Ludwig-Maximilians-Universitat Munchen, Chemistry Klapoetke, Thomas; LMU, Chemistry Lenz, Tobias; Ludwig-Maximilians-Universitat Munchen, Chemistry Rösch, Markus; Ludwig-Maximilians-Universitat Munchen, Chemistry Lommel, Marcus; Ludwig-Maximilians-Universitat Munchen, Chemistry Wurzenberger, Maximilian; Ludwig-Maximilians-Universitat Munchen, Chemistry

ARTICLE

Nitratoethyl-5*H*-tetrazoles: Improving Oxygen Balance through Application of Organic Nitrates in Energetic Coordination Compounds

Received 00th January 20xx,
Accepted 00th January 20xx

DOI: 10.1039/x0xx00000x

Michael S. Gruhne, Tobias Lenz, Markus Rösch, Marcus Lommel, Maximilian H. H. Wurzenberger, Thomas M. Klapötke, Jörg Stierstorfer*

1- and 2-Nitratoethyl-5*H*-tetrazole (1-NET, 2-NET) were prepared through nitration of the respective alkyl alcohol using 100% nitric acid. A mixture of 1- and 2-hydroxyethyl-5*H*-tetrazole was obtained after alkylation of 1,5*H*-tetrazole. Also, a one-pot synthesis for 1-hydroxyethyl-5*H*-tetrazole was invented enabling a selective preparation of 1-NET. Both organic nitrates were characterized by ^{1}H, ^{13}C, and ^{1}H ^{15}N HMBC NMR spectroscopy. In addition, calculations using the Hirshfeld method and the EXPLO5 code were performed. Principally, 20 energetic coordination compounds involving the d-metals Mn, Cu, Zn, and Ag, each structurally characterized by low temperature single crystal X-ray diffraction, were prepared based on 1-NET and 2-NET. Of these complexes, 18 were obtained as pure bulk material, and therefore, characterized toward impact, friction, and ball drop impact sensitivity, as well as electrostatic discharge and thermal stability using differential thermal analysis. Hot plate and hot needle tests were performed mostly showing strong deflagrations making the complexes candidates for green combustion catalysts. Furthermore, successfull PETN initiation experiments were carried out for several complexesand all ECCs were investigated in laser ignition experiments.

Introduction

Ever since the first energetic materials were discovered, research is focused on the improvement of their properties. The explosives widely used today, are tailored to the specific application in terms of power, sensitivity, and stability while being cost efficient.[1] In recent years, there has been a worldwide increase in the demand for environmentally friendly and sustainable materials in every area, including the field of energetic materials.[2] Additionally, regulations such as the REACH directive of the European Union or similar regulations of the U.S. Environmental Protection Agency put pressure on the search for suitable substitutes. In the field of primary explosives commonly used, heavy metal-based lead azide and lead styphnate are harming the user and the environment especially when utilized over a long time.[3] These two lead salts are therefore classified as substances of very high concern (SVHCs).[4]

In the search for new compounds, great attention is now paid on an environmentally friendly production chain while still having a cost-efficient synthesis and long-term stability.[5] The nitrogen-rich tetrazole moiety has proven to be a chameleon for energetic materials.[6] The simplest representative, 1,5*H*-tetrazole, shows sensitivity toward impact due to its high nitrogen content of 80%, but is also a common reactant due to its straightforward preparation.[7] Regarding its derivatives, 1-ethyl-5*H*-tetrazole[8] has proven to be a suitable building block. This structural element has already been successfully used for the introduction of various energetic groups, such as an azido[9] or trinitromethyl group.[10] Also the synthesis of haloethyl[11] and hydroxyethyl[9] tetrazole is described. An overview on the 1-ethyl-5*H*-tetrazole derivatives, already known in the literature together with unknown representatives of this group, is displayed in Chart 1.

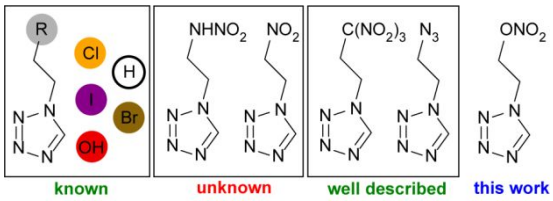

Chart 1. Outline on the tetrazole derivatives based on 1-ethyl-5*H*-tetrazole.[8–11] Corresponding 2-ethyl-5*H*-tetrazoles and especially the 2-nitratoethyl-5*H*-tetrazole, which is also part of this work, are not shown here.

The ethylene group is favourable because of its easy accessibility from the ethylamine hydrochlorides or halides. These starting materials are usually available for purchase at low cost and, with the exception of the trinitromethyl derivative, make the compounds shown in Chart 1 easily accessible.[8–11]

The reason for the preparation of functionalized tetrazoles is not just to fulfil the need for more nitrogen-rich compounds. They also serve to further explore the concept of energetic

Department of Chemistry, Ludwig-Maximilian University of Munich, Butenandtstr. 5–13, D-81337 Munich, Germany. E-mail: jstch@cup.uni-muenchen.de; http://www.hedm.cup.uni-muenchen.de; Fax: +49-89-2180-77007

† Electronic Supplementary Information (ESI) available. See DOI: 10.1039/x0xx00000x

coordination compounds (ECCs). The approach here is to adjust the properties of the resulting complex as desired by varying the parameters of central metal, anion, or ligand.[12] A variation of the substitute on the alkyl chain of the 1-ethyl-5*H*-tetrazole building block, for example, affects solubility, performance, and thermal stability of the ECCs. In every case anion and central metal (here Mn, Cu, Zn, and Ag) also influence the complex's behaviour. However, in this work focus is put on the introduction of an organic nitrate function into the building block to study its effects on the coordination compound.

Organic nitrates are useful for lowering the compounds water solubility, while increasing the oxygen balance.[13] As of today, only two tetrazole derivatives with a nitratoethyl group at the N1 position are known.[14,15] Both molecules, displayed in Chart 2, are not suitable for the use as ligands in promising ECCs. The amino group in the structure on the left, for example, is leading to sterically demanding coordination geometries likely leading to the inclusion of aqua ligands, lowering the performance.[16] Nitrimino groups on the other hand are highly acidic, making them more likely to serve as anionic ligands.[15,17]

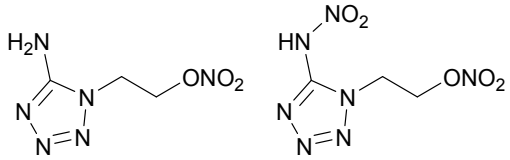

Chart 2. Literature known 1-nitratoetyhltetrazole derivatives.[14,15]

Therefore, in this work focus was put on the preparation of 1- and 2-nitratoethyl-5*H*-tetrazole (1-NET, 2-NET). The resulting coordination compounds show an increased oxygen balance, making them interesting for the use as energetic combustion catalysts in air bag systems or solid rocket propellants as a potential alternative to basic copper nitrate (BCN).[18]

Results and Discussion

CAUTION! *All investigated compounds are potentially explosive energetic materials (the majority of the compounds lie in the range of primary explosives!), which show increased sensitivities toward various stimuli (e.g., elevated temperatures, impact, friction, or electrostatic discharge). Therefore, proper security precautions (safety glasses, face shield, earthed equipment and shoes, leather jacket, Kevlar gloves, Kevlar sleeves, and ear plugs) have to be worn while synthesizing and handling the described compounds.*

Synthesis of the Ligands

Like most tetrazole derivatives, the ligands can be synthesized in two ways. The first strategy, already described by Gaponik *et al*., involves the reaction of 2-aminoethanol or the respective hydrochloride together with triethyl orthoformate and sodium azide, yielding only the 1*H*-substituted derivative **3a** (Scheme 1).[8] However, workup by complexation and subsequent breakdown of the complex with hydrogen sulphide is suggested.

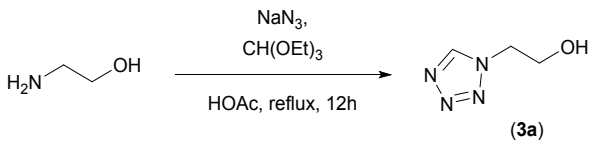

Scheme 1. Synthesis of compound **3a** starting from 2-aminoethanol.

Since the complicated processing of the raw material makes an industrial scale synthesis less promising, the authors have worked out another synthetic pathway toward 1-hydroxyethyl-5*H*-tetrazole (**3a**). As it is assumed that the use of alcohol derivatives together with triethyl orthoformate leads to undesired alkylation products, a modified synthesis of Bays *et al*. was applied.[19] Here, the introduction of a protective group prevents the formation of by-products (Scheme 2). The reaction of 2-aminoethanol hydrochloride with acetic anhydride gave **1** in good yields up to 75%. Subsequently a ring closure reaction was performed resulting in compound **2** in the form of colourless crystals (Yield: 61%). This contradicts literature data, describing the substance as a pale-yellow oil.[19] After reacting compound **2** with concentrated hydrochloric acid, 1-hydroxyethyltetrazole (**3**) was obtained in the form of a colourless solid (Yield: 93%).

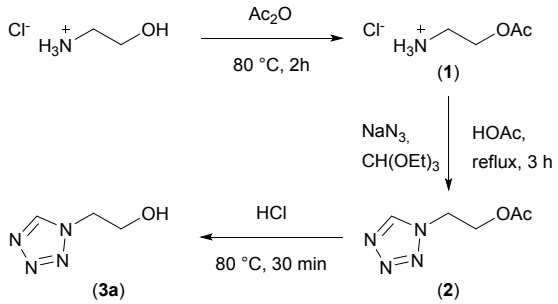

Scheme 2. Synthesis of 1-hydroxyethyltetrazole (**3a**) using acetic anhydride.

The steps can be carried out sequentially (overall yield: 26%), or in an industrially valuable one-pot synthesis, resulting in an overall yield of 75%. For this purpose, acetic acid formed during the reaction of 2-ethanolamine and acetic anhydride was not removed in the first step. The reaction was cooled down to 40 °C and triethyl orthoformate followed by sodium azide was added. After the addition of further acetic acid, the mixture is refluxed. Subsequently, concentrated hydrochloric acid was added to the hot solution and heating is continued for 30 min. All solvents were removed under reduced pressure and the remaining residue was extracted with hot acetone. The solvent was removed under reduced pressure and the product was dried under high vacuum affording compound **3a** as colourless crystals.

To also obtain 2-hydroxyethyl-5*H*-tetrazole, a classic alkylation, as the second synthetic strategy for derivatization of tetrazoles, was applied. A reaction of chloroethanol with 1,5*H*-tetrazole involving a base resulted in a mixture of the two isomers **3a** and **3b** (Scheme 3) in a 1:1 ratio (Yield: 88%).[20] No separation of the products was carried out.

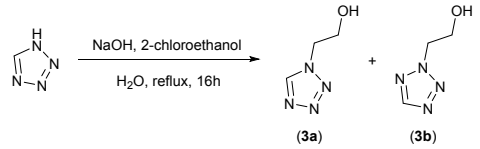

Scheme 3. Reaction of 1,5*H*-tetrazole with 2-chloroethanol.

The nitration of both, the isomeric mixture, as well as pure compound **3a**, was carried out by adding the alcohol to fuming nitric acid. The reaction of the pure 1-isomer with neutralization and extraction yielded compound **4** (Yield: 73%). In case of the isomeric mixture column chromatography with a solvent gradient was used to separate the ligands **4** and **5** (Yield **4**: 45%, Yield **5**: 43%) (Scheme 4). Compound **5** can be further purified by sublimation, but separation of the isomers is not possible with this method.

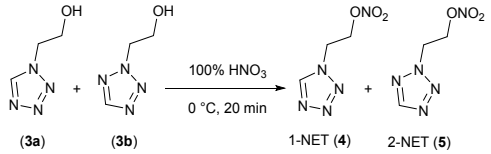

Scheme 4. Nitration of 1-hydroxyethyl-5*H*-tetrazole (**3a**) and 2-hydroxyethyl-5*H*-tetrazole (**3b**).

Analysis of the Ligands

The isomers, thus obtained, were distinguished by infrared spectroscopy (IR) as well as by proton, carbon, and nitrogen NMR spectroscopy. The isomer distribution can easily be followed by integration of the ^{1}H resonances. Furthermore, ^{1}H-^{15}N-HBMC spectra were measured. In these two-dimensional coupled spectra of the tetrazole derivatives **4** and **5**, ^{2}J and ^{3}J couplings between nitrogen and hydrogen are measured. This allows a clear assignment of the isomers (Figures 1 & 2). In advance, compound **5** is analyzed by one dimensional ^{15}N NMR to clarify the superimposed shifts at about −62 ppm (Figure 2, top). The HMBC method used is only showing nitrogen atoms that have a finite ^{1}H, ^{15}N coupling (> 1 Hz) to an immobile hydrogen. This is the case here for all nitrogen atoms. In addition to the simpler atom assignment due to the coupling, the measurement time is many times shorter than for traditional ^{15}N NMR measurements. Additional 14N NMR shifts can be found in the ESI.†

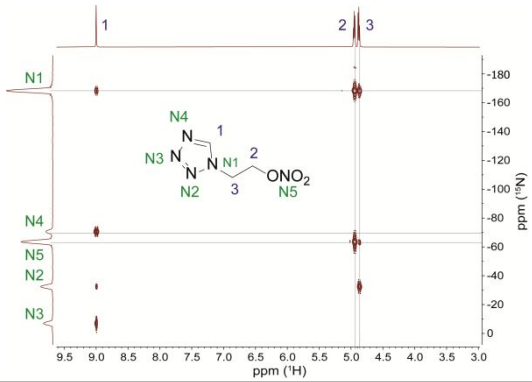

Figure 1. Two-dimensional ^{1}H-^{15}N-HMBC NMR spectra of **4** (MeCN-d_3, 25 °C): δ (ppm) = −7.0 (N3), −32.4 (N2), −63.4 (N5), −70.5 (N4), −168.2 (N1).

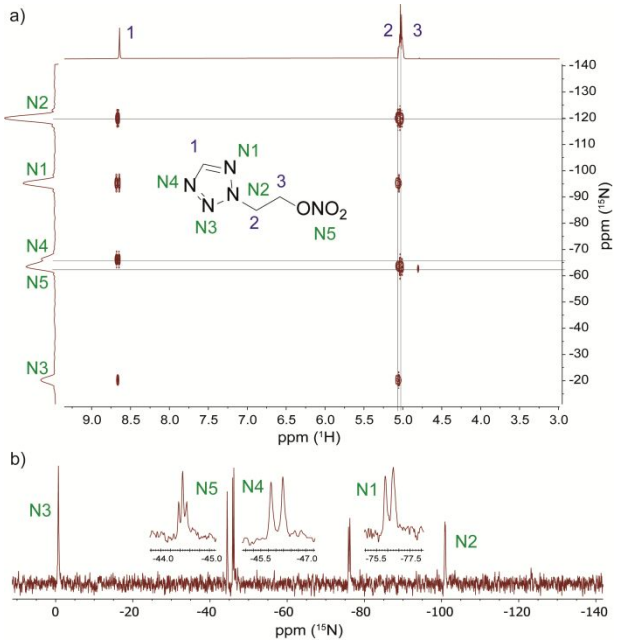

Figure 2. a) Two-dimensional ^{1}H-^{15}N-HMBC NMR spectra of **5** (acetone-d_6, 25 °C): δ (ppm)= −2.0 (N3), −63.5 (N5), −66.4 (N4), −95.3 (N1), −120.1 (N2); **b)** ^{15}N NMR spectra of **5** (acetone-d_6, 25 °C)

The crystal structures of the precursor **2** (Figure S1, ESI†) together with the structures of both nitratoethyl-5*H*-tetrazoles were determined using low temperature single crystal X-ray diffraction (Figure 3). Compound **4** crystallizes in the monoclinic space group $P2_1/n$ and possesses an asymmetric unit of two slightly different ordered molecules of 1-NET. Therefore, the unit cell is built up by eight formula units and shows a calculated density of 1.619 g cm^{-3} at 105 K. In contrast, the isomeric compound **5** crystallizes in the orthorhombic space group $Pna2_1$. The unit cell contains only four formula units and shows a slightly lower density of 1.584 g cm^{-3} at a temperature of 128 K. The bond distances and angles are similar in both molecules as well as comparable to literature known tetrazole derivates and organic nitrates.

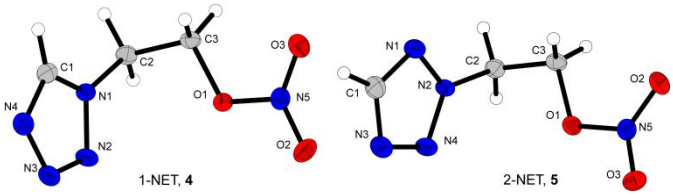

Figure 3. Formula units of 1-NET (**4**) displayed on the left and 2-NET (**5**) on the right. Selected bond lengths (Å) of **4**: N1–C1 1.334(2), N3–N2 1.2978(19), N4–N3 1.359(2), O1–C3 1.4576(17), O1–N5 1.3927(17), O2-N5 1.2038(18). Selected bond lengths (Å) of **5**: N1–C1 1.327(4), N3–N2 1.326(4), N4–N3 1.318(4), O1–C3 1.456(4), O1–N5 1.394(3), O2-N5 1.216(4). Selected bond angles (°) of **4**: N4–C1–N1 109.32(14), N4–N3–N2 111.18(12), N1–C2–C3 111.19(12), C3–O1–N5 113.22(10), O1–N5–O2 113.09(13), O2–N5–O3 128.78(15). Selected bond angles (°) of **5**: N4–C1–N1 113.2(3), N4–N3–N2 106.1(3), N2–C2–C3 111.5(3), C3–O1–N5 114.1(2), O1–N5–O2 118.0(3), O2–N5–O3 129.2(3).

Crystalline material of the ligands was analysed for their sensitivity toward impact and friction according to the "UN declaration of dangerous goods" on a BAM drop hammer and friction tester.[21,22] The hard and brittle crystals of **5** (*IS* = 2 J), are more sensitive toward impact than the plate like and ductile crystals of **4** (*IS* = 10 J). Both ligands are insensitive towards friction (*FS* > 360 N).

Hirshfeld surfaces of 1-NET (**4**) and 2-NET (**5**) were generated, and the intermolecular atom interactions were calculated based on crystallographic data and visualized in the Figure S8 (ESI†).[23] Attractive and repulsive interactions are comparable for both molecules and therefore the exact location of the interactions in the crystal are of more importance. To investigate the location of the respective interaction, structural elements were investigated (Figure 4). The strong interactions, visible as red dots on the Hirshfeld surface (Figure S8, ESI†), are analysed and interactions are visualized in the structural elements. It becomes clear that compound **4** is arranged in layers. These layers have an outer part (green, N–H) and a rigid inner part (grey, nitrato-nitrato, O-H). The layers among themselves are only weakly connected (orange, N-N (π), H–H). It is assumed that these properties are responsible for the ductile, layered physical character. In contrast, compound **5** is largely dominated by hydrogen bonding in every direction and cannot be divided in layers.

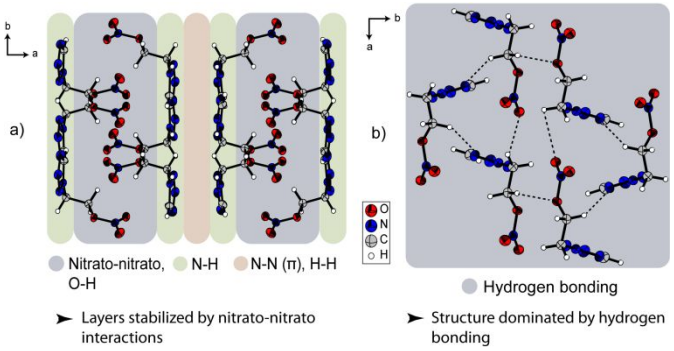

Figure 4. a) Structural elements of 1-NET (**4**) along the *c*-axis; **b)** Structural elements of 2-NET (**5**) along the *c*-axis. The areas showing the same interactions are marked and the type of interaction is noted below the respective structure.

The crystal is thus fixed in all spatial directions and is clearly more rigid, which is also consistent with the physical properties. With this information, one could explain the lower sensitivity of compound **4**, through its layer like structure.[24] Regarding the low sensitivity toward friction we believe, that the heat generated through the applied friction force leads to a melting and therefore desensitizing of the samples (liquid samples are often less sensitive towards friction).[6] It is questionable if the impact is causing the solid sample to detonate or if a melting occurs beforehand.[25]

The heat of formation of **4** and **5** was calculated using the atomization method (Gaussian CBS-4M electronic enthalpies) and the detonation parameters were calculated using the EXPLO5 V6.05 code (Table 1).[26] Additional information on the calculations is given in the ESI† (Tables S7 & 8). The heat of formation of 1-NET (**4**) is 27 kJ mol^{-1} higher than of 2-NET (**5**). This leads to a detonation velocity of 7583 m s^{-1} for compound **4**, and a slightly lower value of 7420 m s^{-1} for compound **5**. In Table 1 the most important physico-chemical and calculated properties of **4**, **5**, and TNT are compared. Although the melting points of **4** and **5** are too close to room temperature to classify the energetic materials as suitable melt castable material, it proofs the compatibility of the tetrazole and the nitrate ester moiety.

Table 1. Physico chemical and calculated properties of **4**, **5,** and TNT.

Compound	**4**	**5**	**TNT**
IS^a [J]	10	2	15
FS^b [N]	> 360	> 360	> 360
$\Omega_{CO2}{}^c$ [%]	−55.31	−55.31	−73.96
$T_{endo}{}^e$ / $T_{exo}{}^f$ [°C]	25 / 168	24 / 188	80 / 290
ρ^g [g cm^{-3}]	1.55	1.57	1.65
$\Delta_f H_m{}^{\circ h}$ [kJ mol^{-1}]	174	147	−59
Detonation parameters calculated with EXPLO5 V6.05 code			
$-\Delta_E U^{\circ i}$ [kJ kg^{-1}]	4861	4689	4406
$T_E{}^j$ [K] ^{h}	3336	3268	3176
$p_{C\text{-}J}{}^k$ [GPa] ^{i}	21.5	20.4	18.3
$V_{det}{}^l$ [m s^{-1}] ^{k}	7583	7420	6798
$V_0{}^m$ [L kg^{-1}] ^{l}	815	818	640

[a]Impact sensitivity (BAM drop hammer, 1 of 6); [b]friction sensitivity (BAM friction tester, 1 of 6); [c]oxygen balance toward CO_2; [e]endothermic peak, which indicates melting; [f]exothermic peak, which indicates decomposition; [g]calculated density at 298 K, [h]calculated enthalpy of formation at 298.15 K, [i]heat of explosion, [j]detonation temperature, [k]detonation pressure, [l]detonation velocity, [m]volume of detonation gases (assuming only gaseous products).

Synthesis of the ECCs

Many complexes based on monotetrazole ligands are already known in the literature.[27–29] However, in addition to their good performance, these usually exhibit very good water solubility, which is generally not desired in the field of energetic materials. To address this problem, a variety of ECCs containing the organic nitrate-based ligands 1-NET (**4**) and 2-NET (**5**) were prepared. The resulting complexes should not only exhibit a reduced solubility, but at the same time maintain their performance.

In a first step, several neutral or cationic coordination compounds based on oxidizing anions like nitrate, dinitramide, chlorate, or perchlorate were formed. The role of the ligand is to tune the energy content and sensitivity of the complex. Due to the bad solubility of the ligand, the sole use of water as a green solvent was not possible. Therefore, acetonitrile, or a combination of water and acetonitrile was applied for the preparation of the coordination compounds **6–13**. Besides rather easily accessible nitrate anion, the dinitramide anion was made accessible using basic copper carbonate and dinitraminic acid, as published in our previous work (Scheme 5).[30] Both metal salts were reacted with stoichiometric amounts of the ligand and crystallized within several days in decent yields up to 96% in the form of single crystals suitable for X-ray diffraction.

Furthermore, the strongly oxidizing chlorate anion was used, as it is also less toxic than the perchlorate anion.[31] In addition to copper(II) chlorate (**8**), the less investigated zinc(II) chlorate (**9**) was also incorporated in an ECC. The respective

metal chlorate was made accessible by a reaction of barium chlorate with the respective sulphate salts (Scheme 6).[31b] Both complexes were obtained in the form of single crystals in high yields (80–84%).

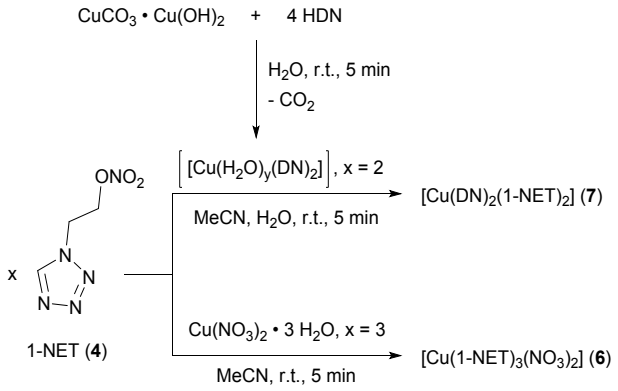

Scheme 5. Preparation of the copper(II) complexes **6** and **7**.

The compounds **10–13** were prepared analogous to the copper(II) nitrate complex **6** by combining solutions of the respective metal salt and stoichiometric amounts of the ligand, each dissolved in acetonitrile (Scheme 6). Whereas the use of manganese(II) and zinc(II) perchlorate only lead to the isolation of a few single crystals, applying 1-NET (**4**) to copper(II) perchlorate gave ECC **11** in a satisfying yield (76%). Using 2-NET (**5**) solely resulted in the copper(II) perchlorate complex **13** (Yield: 89%). Single crystals suitable for X-ray diffraction were not obtained. Applying 2-NET (**5**) to copper(II)nitrate, dinitramide or different perchlorate salts like manganese(II) or zinc(II) was not successful. The use of iron(II) perchlorate as a building block did also not result in any isolable complexes in either case.

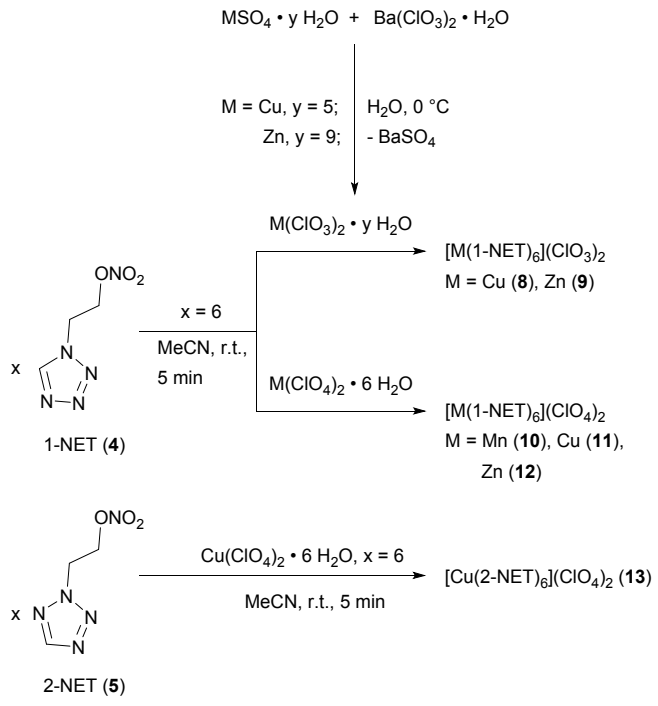

Scheme 6. Synthesis of the coordination compounds **8–13**.

Besides the use of neutral nitrogen-rich ligands as a means of enhancing performance in nitrate or perchlorate complexes, the concept of ECCs also allows a stabilization of highly sensitive metal salts like copper(II) azide or silver(I) fulminate (Scheme 7). Both synthetic strategies were recently published by our group.[32,33] To obtain the copper(II) azide complex **14**, the respective copper(II) sulphate complex is formed *in situ* and further reacted with an aqueous solution of sodium azide. Since the coordination positions remain occupied by the ligands, the formation of pure copper azide is avoided. The complex is formed immediately and precipitates directly and can be filtered off in a very good yield (82%). An elemental analysis pure preparation of compound **15** was not possible using this method, as most likely a side species is formed. Single crystal growth of **14** and **15** was achieved by performing layering experiments. Whereas handling of an extremely sensitive species could be avoided during the preparation of **14** and **15**, pure silver fulminate must be used for obtaining ECC **16a**. The silver salt was dissolved in a warm mixture of water and acetonitrile and an excess of ligand in acetonitrile was added. Single crystals suitable for X-ray diffraction were obtained after two days (Yield: 43%). Leaving compound **16a** in its mother liquor for four weeks is resulting in single crystals of the thermodynamic product **16b**.

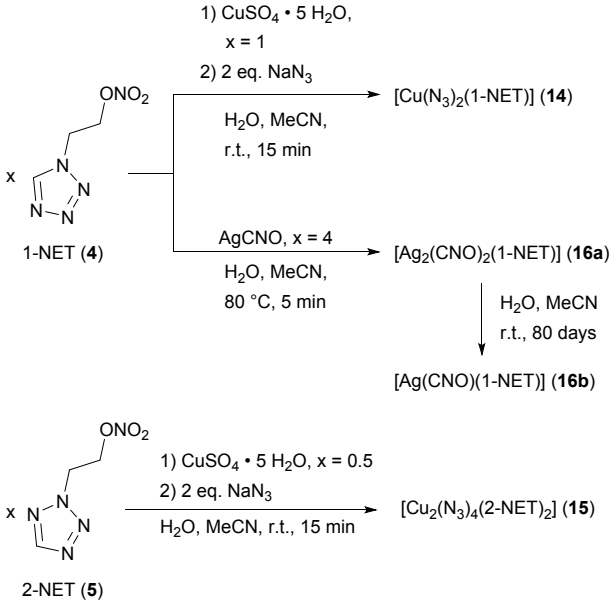

Scheme 7. Stabilization of copper(II) azide and silver(I) fulminate using 1-NET and 2-NET.

Another well-studied system is that of the trinitrophenolate anions, each of which provides different properties to the respective complex depending on the number of hydroxy groups.[29] The compounds **17–22** were prepared in a straight forward manner by the reaction of basic copper carbonate with stoichiometric amounts of the respective acid in boiling water (Schemes 8 & 9). Subsequently, the ligand dissolved in small amounts of acetonitrile was added. Single crystal formation started within one day, depending on the amount of water

used, in sufficient to high yields (68–88%). In case of compound **18a** no single crystals suitable for X-ray diffraction were obtained but its composition could be verified by elemental analysis. Instead, recrystallization from hot water afforded single crystals of **18b**. Unfortunately, an elemental analysis pure isolation of **18b** was not possible.

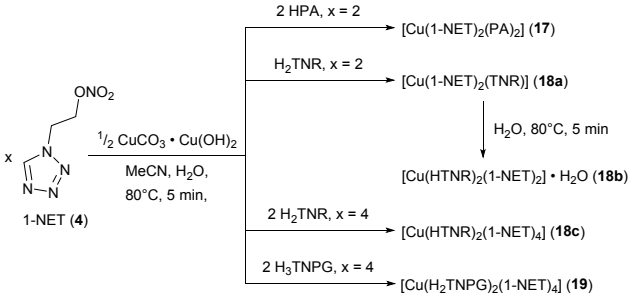

Scheme 8. Preparation of copper(II) picrate (PA), styphnate (HTNR/TNR) and 2,4,6-trinitrophloroglucinol-based (HTNPG/H_2TNPG) complexes of 1-nitratoethyltetrazole (1-NET, **4**).

By variation of the number of anions added to one equivalent of basic copper carbonate different states of deprotonation of the styphnate ($HTNR^-$and TNR^{2-}, Scheme 8) or trinitrophloroglucinate (H_2TNPG^- and $HTNPG^{2-}$, Scheme 9) anions could be obtained. In case of compound **22c**, the addition of 6 equivalents of 2-NET led to the formation of a co-crystalline species, resulting in a total of three different species based on trinitrophloroglucinol. Each of these ECCs was obtained pure according to elemental analysis.

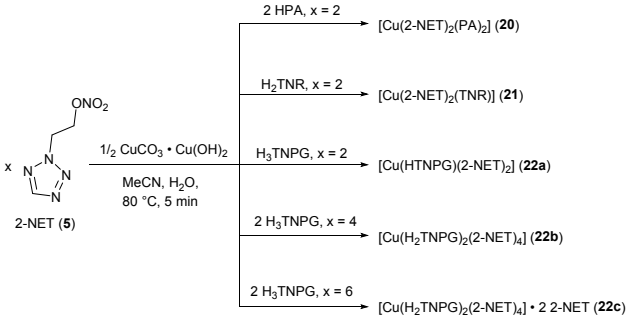

Scheme 9. Reaction of basic copper(II) carbonate with several trinitrophenole derivatives and subsequent application of 2-NET (**5**).

Except side species **18b**, all coordination compounds crystallized without the inclusion of water and were isolated directly from the mother liquor. The crystalline materials were filtered off, washed with small quantities of ice-cold ethanol, and then dried in air overnight.

Crystal Structures of the ECCs

The ECCs **6**–**12** and **14**–**22**, were examined by low-temperature single crystal X-ray diffraction. In case of the compounds **9** and **22b** the measurements allow an indication of the most likely composition, but finalization of the data sets was not possible due to the highly disordered nitratoethyl moieties. Together with compounds **13** and **18a** in which case no single crystals were obtained, the complexes' composition was finally confirmed by elemental analysis. Details on the structures of compounds **2**, **10**, **12**, **15**, **18b**, **18c**, **19**, **21**, **22a**, and **22c** (Figures S1–7, ESI^+) are given in the Supporting Information, together with the measurement and refinement data of all experiments (Tables S1–S6, ESI^+). The crystal datasets were uploaded to the CSD database and can be obtained free of charge.[34] All copper(II) complexes, except the nitrato (**6**), and dinitramido (**7**) ECCs, show octahedral coordination spheres around the copper(II) centers. Therefore, typical Jahn-Teller distortions along the respective O–Cu–O or N–Cu–N axes can be observed. Except for ECC **16b**, the ligands are solely coordinating via the N4 nitrogen atom of the tetrazole rings.

The copper(II) nitrate complex **6** crystallizes in the monoclinic space group $P2_1/c$ with four formula units per unit cell. The compound possesses a calculated density of 1.888 g cm^{-3} at 99 K. The coordination sphere could either be interpreted as distorted fivefold trigonal bipyramidal (N9–Cu1–O10 147.87(10)°, O10–Cu1–O13 80.22(8)°), or as distorted seven fold pentagonal bipyramidal (N9–Cu1–O11 96.37(9)°, O11–Cu1–O10 51.93(8)°) depending on whether the longer Cu–O bonds between central metal and nitrato ligands are included (Cu1–O11 2.695(2) Å, Cu1–O14 2.583(2) Å). In every case, the equatorial positions are occupied by the anionic nitrato ligands, and one ligand moiety (Figure 5).

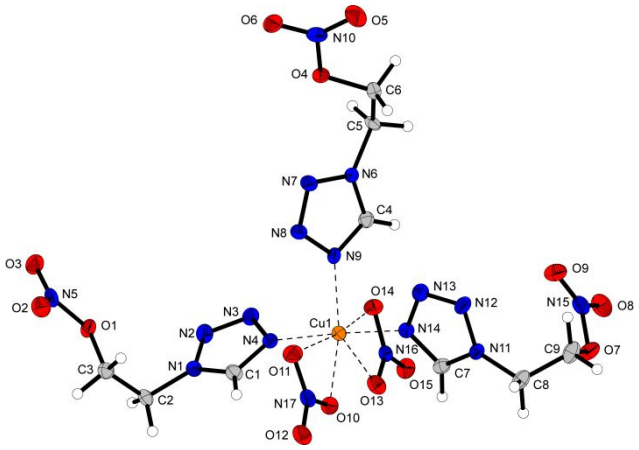

Figure 5. Formula unit of $[Cu(1\text{-}NET)_3(NO_3)_2]$ (**6**). Selected bond lengths (Å): Cu1–N9 2.028(3), Cu1–N4 1.973(3), Cu1–N14 1.987(3), Cu1–O10 2.117(2), Cu1–O13 2.268(2). Selected bond angles (°): N9–Cu1–N4 93.87(10), N9–Cu1–N14 89.14(10), N14–Cu1–N4 174.78(11), N4–Cu1–O11 86.03(9).

The dinitramide complex **7** crystallizes in the monoclinic space group $P2_1/n$ with two formula units per unit cell. The complex shows a high density of 1.953 g cm^{-3} at 102 K, with only the copper azide and silver fulminate complexes possessing higher densities. The coordination sphere is built up by two ligand moieties and two coordinating dinitramido anions (Figure 6). This rather uncommon built up was already observed one time by our group having 1-azidoethyl-5*H*-tetrazole as ligand.[30] One way of explaining the complexes' coordination geometry is by two square planar spheres by either the oxygen atoms of the anion or the nitrogen atoms of anion and ligand. Another possible coordination geometry might be a distorted

hexagonal bipyramidal. Also, worth It should be pointed out that in each case the extremely long Cu-O bonds were included. (Cu1–O1 2.8715(17) Å, Cu1–O4 2.8287(17) Å). Therefore, no clear Jahn-Teller distortion can be observed, but a strongly distorted dinitramide anion is evident (O7–N8–N7–O5 25.19(17)°, O6–N8–N6–N7 150.45(16)°).

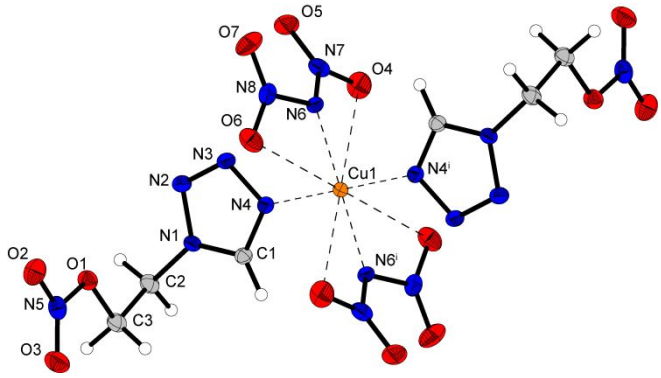

Figure 6. Coordination environment of $[Cu(DN)_2(1\text{-NET})_2]$ (**7**). Selected bond lengths (Å): Cu1–N6 1.9978(17), Cu1–N4 1.9735(17). Selected bond angles (°): N4–Cu1–N6 90.02(7), O4–Cu1–N4 90.33(6), O6–Cu1–N4 102.57(6), O6–Cu1–N6 49.13(6), O4–Cu1–N6 49.33(6), N6–N8–O6 111.96(17), N6–N7–O4 110.25(17). Symmetry code: (i) 1–x, 1–y, 1–z.

The copper(II) chlorate complex **8** crystallizes in the monoclinic space group *Cc* and the unit cell consists of four formula units. The compound's density of 1.689 g cm^{-3} (at 100 K) is slightly lower than the density observed for the corresponding perchlorate complex **11**. The octahedral coordination sphere is built up by six ligand moieties, whereas some nitrato-groups had to be split due to disorder and are therefore not refined anisotropic. The metal perchlorate complexes **10–12** crystallize isotypically in the triclinic space group *P*–1 with one formula unit per unit cell. The observed densities differ only slightly, with the copper coordination compound showing the highest value (**10** (Mn): 1.681 g cm^{-3} at 123 K; **11** (Cu): 1.727 g cm^{-3} at 114 K; **12** (Zn): 1.719 g cm^{-3}). Each compound shows an octahedral coordination sphere built up by six moieties of 1-NET (**4**), whereas only **11** shows a Jahn-Teller distortion due to its d^9 configuration (Figure 7).

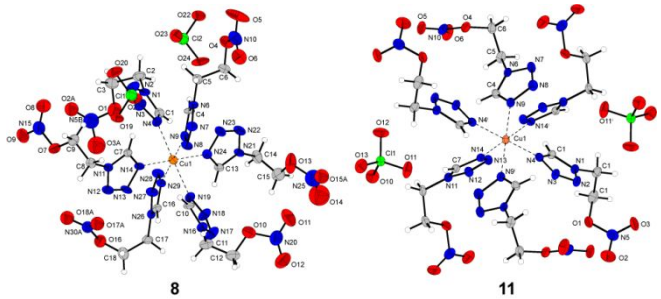

Figure 7. Formula units of $[Cu(1\text{-NET})_6](ClO_3)_2$ (**8**) and $[Cu(1\text{-NET})_6](ClO_4)_2$ (**11**). Selected bond lengths (Å) of **8**: Cu1–N4 2.371(8), Cu1–N9 2.048(8), Cu1–N14 2.046(7). Selected bond lengths (Å) of **11**: Cu1–N4 2.022(3), Cu1–N14 2.035(3), Cu1–N9 2.338(3). Selected bond angles (°) of **8**: N4–Cu1–N9 86-1(3), N4–Cu1–N14 92.8(3), N9–Cu1–N14 88.7(3). Selected bond angles (°) of **11**: N9–Cu1–N4 89.48(11), N9–Cu1–N14 88.66(10), N14–Cu1–N4 91.60(11). Symmetry codes of **11**: (i) 1–x, 1–y, 1–z.

Copper(II) azide complex **14** crystallizes in the form of brown plates in the triclinic space group *P*–1. The asymmetric unit consists of two molecular units, whereas the molecular unit is built up by one tetrazole moiety per copper(II) azide. This coordination geometry has already been observed in previous studies.[32] The unit cell contains four formula units and shows the highest density of all investigated copper complexes (1.985 g cm^{-3} at 173 K). Each copper centre is surrounded by a strongly distorted octahedral coordination sphere (N11–Cu1–N11^{i} 77.11(13)) with the 1-NET ligands in equatorial positions (Figure 8, part A). The remaining coordination sites are occupied by azido ligands. In addition to that the azide anion show a bridging behaviour, further linking the copper centres in various ways. Two of the anions show the same binding behaviour and bridge exclusively to the same neighbouring copper centres. This binding behaviour, shown in part C of Figure 8, leads to the formation of dimers. The remaining equatorial coordinating azide ion, as well as both moieties in axial position, exhibit a bridging behaviour as shown in part B of Figure 8. This further linking of the metal centres leads to the formation of a two-dimensional polymeric network, as displayed in part D (Figure 8).

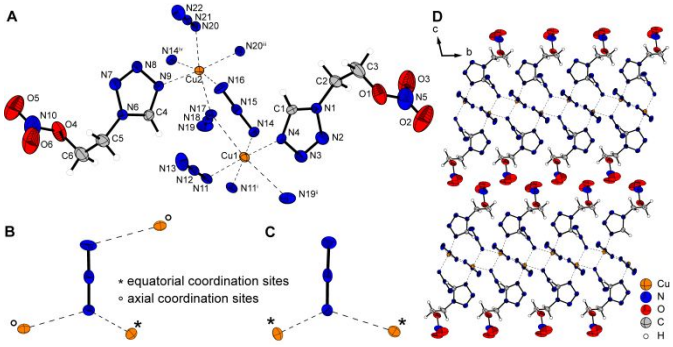

Figure 8. A: Coordination environment of the copper(II) azide dimer **14**. Selected bond lengths (Å): Cu1–N17 2.497(3), Cu1–N19^{ii} 2.683(3), Cu2–N14^{iv} 2.534(3), Cu2–N16 2.715(3). Selected bond angles (°):N14–Cu1–N19^{ii} 84.62(10), N11^{i}–Cu1–N4 95.86(11), N11–Cu1–N14 94.55(12), N9–Cu2–N20 95.15(11), N17–Cu2–N16 86.55(10), N16–Cu2-N20 86.85(19), N16–Cu2–N14^{iv} 170.95(10), N20–Cu2–N17 169.31(11). Symmetry codes: (i) 1–x, 1–y, 1–z; (ii) –1+x, y, z; (iii) 2–x, 2–y, 1–z; (iv) 1+x, y, z. **B** & **C**: Coordination modes of the azide anions. **D**: Polymeric structure of compound **14.**

The silver complex **16a** crystallizes in the form of colourless plates in the monoclinic space group *I*2/a. The unit cell consists of eight formula units and shows the highest density of all investigated compounds with 2.718 g cm^{-3} at 104 K. A molecular unit consists of one 1-NET per two silver fulminate moieties. In addition to the formation of argentophilic Ag–Ag interactions, all centres within the cluster are further linked to each other by the fulminate anions. Two identical cations are bridged by two anions, one via the carbon of one fulminate ligand and the other via the oxygen atom of the other fulminate ligand, in alternating order forming twofold coordinated silver chains. This 1D polymeric chain is further coordinated by 1-NET ligands which shifts the linear 2-fold coordination of the silver atoms to a distorted tetrahedral coordination. The resulting fourfold coordination environment around each silver cation

has already been observed for silver(I) fulminate complexes based on monotetrazole ligands.[33]

The fulminato complex **16b**, based on the same ligand as complex **16a**, on the other hand crystallizes in the monoclinic space group $P2_1/c$ with four formula units. The calculated density of 2.337 g cm^3 at 173 K is lower than the one determined for **16a**. The molecular formula in this case consists of only one silver fulminate moiety per 1-NET ligand. Also, the silver atoms are coordinated different (Figure 9, bottom). In compound **16b** each silver atom shows only a six-fold coordination sphere, whereas no Ag–O bonds were found. Instead, bridging tetrazole ligands were observed. Every moiety of 1-NET is binding via its N4 nitrogen atom together with its N3 position, which is a rather uncommon behaviour of tetrazoles in ECCs. This linking is further connecting the Ag-Ag chains formed by the fulminato ligands, leading to 2D polymeric sheets.

Overall, both silver fulminate complexes based on 1-NET (**4**) form two dimensional polymeric networks, while the sum formula and the structure of these networks are very different.

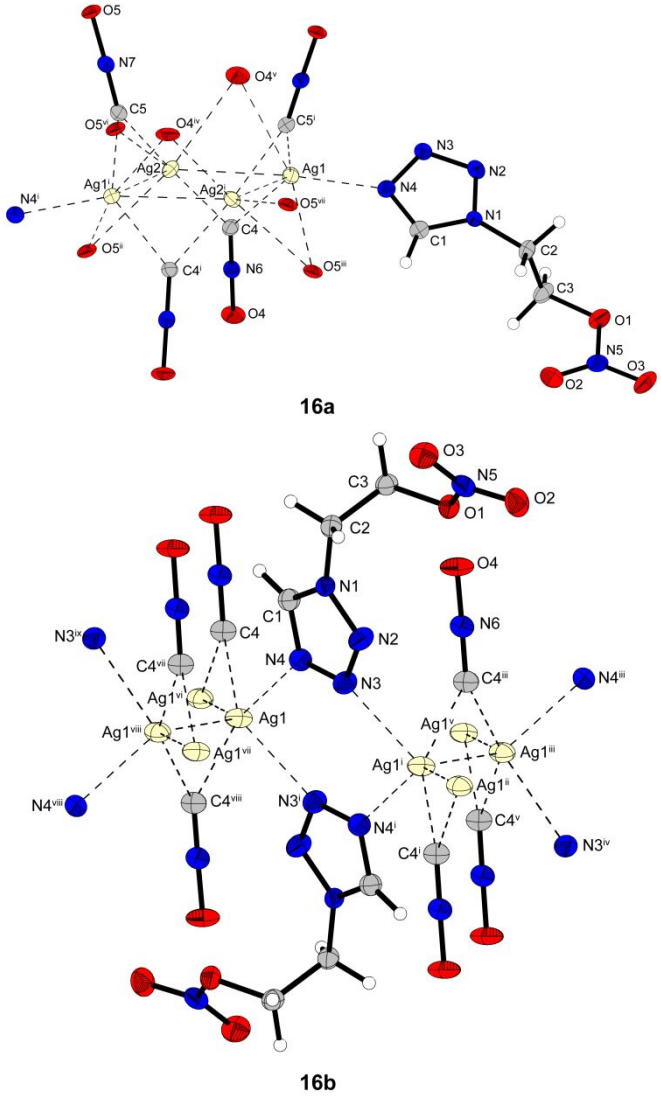

Figure 9. Extended molecular units of $[Ag_2(CNO)_2(1\text{-NET})]$ (**16a**) and [Ag(CNO)(1-NET)] (**16b**). Selected bond lengths (Å) of **16a**: Ag1–N4 2.291(3), Ag2–O5 2.501(3), Ag1–C4 2.236(3), Ag2–C4 2.195(4), Ag1–O4 2.893(3), Ag2–O4 2.846(3), Ag1–C5 2.242(4), Ag2–C5 2.200(4), Ag1–O5 2.698(2), Ag2–O5 2.703(2). Selected bond lengths (Å) of **16b**: Ag1–Ag1^{vi} 3.0106(2), Ag1–C4 2.184(2), Ag1^{vi}–C4 2.247(2), Ag1–N4 2.4260(18), Ag1–N3 2.4692(19). Selected bond angles (°) of **16a**: Ag2–Ag1–N4 161.47(8), Ag1–Ag2–O5 126.02(6), Ag2-Ag1–Ag2 67.284(13), Ag1–Ag2–Ag1 112.694(13), Ag2–C4–Ag1 77.89(11), Ag1–O5–Ag2 64.53(5). Selected bond angles (°) of **16b**: Ag1^{vi}–Ag1–C4 48.10(6), Ag1-C4–Ag1^{vi} 85.59(7), N4-Ag1–N3^{i} 103.46(6), N4–Ag1–C4^{viii} 106.50(7), N3–Ag1–C4^{viii} 82.16(7). Symmetry codes of **16a**: (i) 1.5−x, y, 1−z; (ii) x, −1+y, z; (iii) 1.5−x, −1+y, 1−z; (iv) 1.5−x, 1+y, 1−z; (v) x, 1+y, z; (vi) 2−x, 2−y, 1−z; (vii) −0.5, 2−y, z. Symmetry codes of **16b**: (i) 1-x, 1-y, 1-z; (ii) x, 1.5−y, −0.5+z; (iii) x, 0.5−y, −0.5+z; (iv) 1x, −0.5+y, 0.5−z; (v) 1−x, −y, 1z; (vi) 1−x, −0.5+y, 1.5−z; (vii) x, 1+y, z; (viii) 1−x, 0.5+y, 1.5−z; (ix) x, 1.5−y, 0.5+z.

Both complexes **17** and **20** based on the picrate anion crystallize with the same molecular formula in the form of green plates or blocks, respectively. However, since both complexes crystallize in different space groups (**17**: monoclinic $P2_1/c$; **20**: triclinic $P\bar{1}$), the unit cell of compound **17** consists of four formula units and the one of **20** is made of one unit Despite this fact, the densities of both complexes are very similar (**17**: 1.852 g cm^{-3} at 173 K, **20**: 1.890 g cm^{-3} at 132 K). The distorted octahedral coordination sphere is, for picrate-based complexes, structured in the expected manner.[27,29] Two ligand moieties are arranged in the equatorial positions together with Cu–O bonds formed by the deprotonated hydroxy groups of the anion (Figure 10). The axial positions are occupied by oxygen atoms of picrate's nitro group next to its hydroxy group.

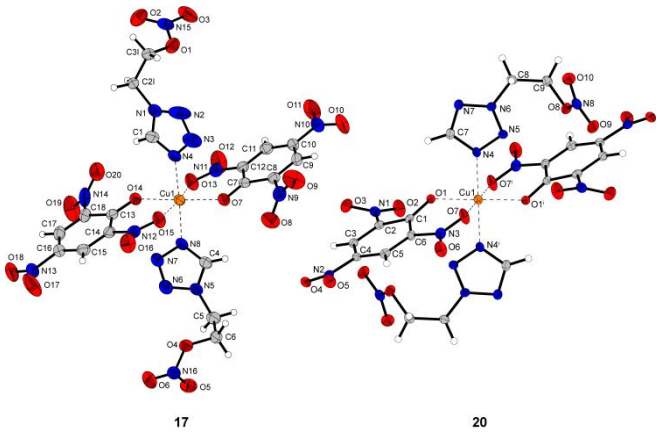

Figure 10. Molecular units of the ECCs **17** and **20**. Selected bond lengths (Å) of **17**: Cu1–N4 1.999(3), Cu1–N8 2.000(3), Cu1–O14 1.919(2), Cu1–O7 1.931(2), Cu1–O13 2.296(2), Cu1–O15 2.412(3). Selected bond lengths (Å) of **20**: Cu1–O1 1.9193(18), Cu1–N4 2.001(2), Cu1–O7 2.430(2). Selected bond angles (°) of **17**: O7–Cu1–O13 81.58(9), O13–Cu1–O14 94.72(9), O14–Cu1–O15 77.39(9), O13–Cu1–N4 88.02(11), N4–Cu1–O15 92.32, N4–Cu1–O14 85.29(10), O14–Cu1–N8 91.67(10). Selected bond angles (°) of **20**: O7–Cu1–O1 76.34(7), O7–Cu1–N4 89.49(8), N4–Cu1–O1 87.10(8). Symmetry code of **20**: (i) 1−x, 2−y, 1−z.

Thermal Stability and Sensitivities Data of the ECCs

Each coordination compound, which could be obtained elemental analysis pure, was investigated by differential thermal analysis (DTA) in the range from 25 to 400 °C at a heating rate of 5 °C min^{-1}. The resulting endothermic events indicating a melting of the respective compound, a loss of ligand, or a phase transition, together with the exothermic events, indicating a decomposition, are listed in Table 2. Plots of every DTA spectrum measured can be found in the ESI^{+} (Figures S20–24). When endothermic events occurred during DTA measurements, thermogravimetry (TG) was applied at a

heating rate of 5 °C min^{-1} in the range of 30 to 400 °C to ensure that only melting of the respective compound occurred. The TG plots of the chlorate and perchlorate complexes **8**, **9**, **11**, and **13** are illustrated in Figure 11. Further spectra can be found in the ESI† (Figures S25 & 26). In case of **16a**, the second endothermic event indicates a loss of ligand according to TG measurements. Since no mass loss has been detected for compound **11**, a phase transformation probably takes place here.

Except the nitrate (**6**, T_{exo} = 196 °C) and the trinitrophenolate based complexes **17** (T_{exo} = 197 °C) and **18a** (T_{exo} = 195 °C), none of the compounds' thermal stability exceeds the free ligands stability. Furthermore, quite low melting points were observed especially for the chlorate and perchlorate complexes **8**, **9**, **11**, and **13**. This is most likely due to the low melting temperatures of the respective ligands (**4**, **5**: T_{endo} ≤ 25 °C). The complexes' low decomposition temperatures are on the one hand again caused by the ligand's properties. Organic nitrates in general are known to possess decomposition temperatures rarely exceeding 180 °C.[35] Therefore, it is to be expected that the compounds exothermic events are within this range. On the other hand, catalytic effects might play a crucial role in the decomposition of the ECCs, further limiting the compounds' thermal stability. Thus, similar effects like those observed in the catalytic decomposition of guanidinium nitrate using BCN, probably occur when the complexes are heated.[18,36]

A detailed look at the compounds' exothermic events reveals some trends already observed for ECCs in the past. For example, complex **11** (T_{exo} = 165 °C) based on the perchlorate anion is among the most thermally stable compounds, whereas the respective copper(II) chlorate **8** complex (T_{exo} = 149 °C) is less stable.[9]

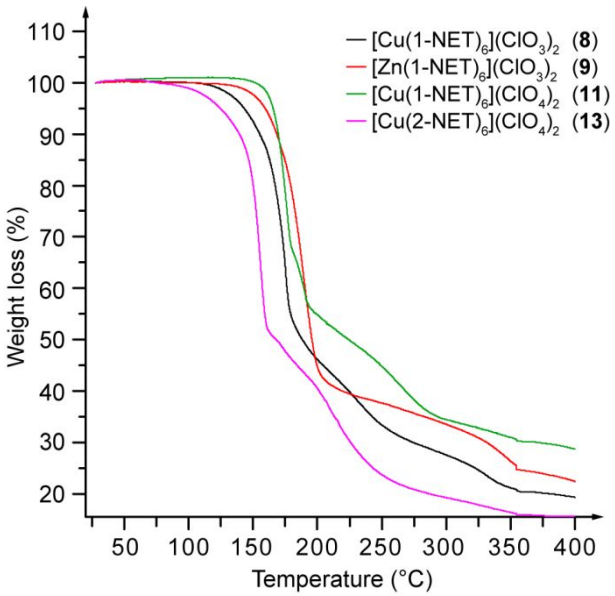

Figure 11. Thermogravimetric measurements of the copper(II) and zinc(II) chlorate complexes **8** and **9** together with the copper(II) perchlorate complexes **11** and **13** in the range from 30 to 400 °C at a heating rate of 5 °C min^{-1}.

Also, the decrease in the thermal stability of the complexes **20** (T_{exo} = 165 °C) to **22c** (T_{exo} = 105 °C) with an increasing number of hydroxy groups is to be expected.[29] The expected trend of improved thermal stability caused by bridging anions (such as TNR^{2-} and $HTNPG^{2-}$) was only observed for complexes **18a** (T_{exo} = 195 °C), **21** (T_{exo} = 161 °C), and **22a** (T_{exo} = 112 °C).[9,29] Previous results suggest that the thermal stability of these complexes should be significantly higher than that of the picrate complexes. The drastically lower decomposition temperature of **13** (T_{exo} = 143 °C) was also surprising. Literature data showed rather similar decomposition temperatures for copper(II) perchlorate complexes based on the respective isomers. The reason for this again appears to be catalytic effects of the central metal on the stability of the organic nitrate of the ligand. Hence, the latest exothermic events were observed for the compounds **6**, **17**, and **18a**. The compounds **16b** (T_{exo} = 102 °C), **22b** (T_{exo} = 105 °C), and **22c** (T_{exo} = 105 °C) showed the lowest thermal stability of all complexes investigated.

In addition to the compound's thermal stability, great emphasis was put on the determination of the compounds' sensitivity toward various external stimuli (e.g., impact, friction, ball drop impact sensitivity, and electrostatic discharge). The classification of the compounds regarding the "UN Recommendations on the Transport of Dangerous Goods" should ensure a safe handling of every ECC investigated. Sensitivity measurements were carried out for the complexes **6**–**9**, **11**, **13**, **14**, and **16**–**22** and the ligands **4** and **5**. A further characterization of coordination compounds which could not be isolated elemental analysis pure was waived. Friction sensitivity (FS) measurements showed that, except picrate complex **17**, every ECC is more sensitive than the respective ligand is by itself. The copper azide **14** is the most sensitive complex (*FS* = 1 N), followed by the copper(II) perchlorate complex **13** (*FS* = 5 N), and the copper(II) dinitramide complex **7** (*FS* = 7 N). This is surprising as compound **13** at the same time possesses one of the lowest melting points. In the case of the compounds **8** (*FS* = 15 N), **9** (*FS* = 14 N), and **11** (*FS* = 25 N) the low melting point is clearly reducing the compounds' friction sensitivity. Also, worth mentioning is the effect of the co-crystallizing 2-NET moieties in compound **22c** on the compound's higher sensitivity toward friction (*FS* = 60 N). Compared to **22b** (*FS* = 324 N), lacking the co-crystallizing 2-NET units, the sensitivity is drastically higher. This contradicts the common assumption that energetic materials are less sensitive by introducing co-crystallizing compounds.[37]

Regarding impact sensitivity (IS) measurements, the effects caused by the low melting points are not as severe as during friction sensitivity measurements. This is reflected by the general impact sensitivity of ≤ 4 J observed for most of the compounds (except **6**, **9**, and **17**). A reason for this might be ignition of the sample through adiabatic compression or hot spot formation within the setup.[25] Also, worth mentioning is, that during impact sensitivity measurements some complexes are tested to be less sensitive than ligand **5** (*IS* = 2 J). The highest impact sensitivity was observed for styphnate **21** (*IS* ≤ 1 J), whereas compound **17** (*IS* = 20 J) showed the lowest sensitivity toward impact.

Table 2. Thermal stability measurements[a] and sensitivities toward various mechanical stimuli.[b]

Compound		T_{endo}[c] (°C)	T_{exo}[d] (°C)	*IS*[e] (J)	*FS*[f] (N)	*ESD*[g] (mJ)	*BDIS*[h] (mJ)
1-NET	**4**	25	168	10	> 360	n.d.	n.d.
2-NET	**5**	24	188	2	> 360	n.d.	n.d.
$[Cu(1\text{-}NET)_3(NO_3)_2]$	**6**	121	196	5	48	1080	14
$[Cu(DN)_2(1\text{-}NET)_2]$	**7**	–	110	2	7	1080	14
$[Cu(1\text{-}NET)_6](ClO_3)_2$	**8**	54	149	2	15	250	55
$[Zn(1\text{-}NET)_6](ClO_3)_2$	**9**	71	154	7	14	750	69
$[Cu(1\text{-}NET)_6](ClO_4)_2$	**11**	70, 117	165	3	25	480	> 200
$[Cu(2\text{-}NET)_6](ClO_4)_2$	**13**	65	143	2	5	1080	55
$[Cu(N_3)_2(1\text{-}NET)]$	**14**	–	122	3	1	14	≤ 4
$[Ag_2(CNO)_2(1\text{-}NET)]$	**16a**	96	123	≤ 1	20	250	8
[Ag(CNO)(1-NET)]	**16b**	67, 102*	102*	9	60	250	83
$[Cu(1\text{-}NET)_2(PA)_2]$	**17**	–	197	20	> 360	480	> 200
$[Cu(1\text{-}NET)_2(TNR)]$	**18a**	–	195	2	96	480	111
$[Cu(HTNR)_2(1\text{-}NET)_4]$	**18c**	–	167	5	96	> 1500	> 200
$[Cu(H_2TNPG)_2(1\text{-}NET)_4]$	**19**	–	108	2	96	1080	> 200
$[Cu(2\text{-}NET)_2(PA)_2]$	**20**	165*	165*	3	192	1080	> 200
$[Cu(2\text{-}NET)_2(TNR)]$	**21**	–	161	≤ 1	80	750	138
$[Cu(HTNPG)(2\text{-}NET)_2]$	**22a**	–	112	4	324	750	> 200
$[Cu(H_2TNPG)_2(2\text{-}NET)_4]$	**22b**	–	105	4	324	750	> 200
$[Cu(H_2TNPG)_2(2\text{-}NET)_4]$ • 2 2-NET	**22c**	92	105	4	60	750	> 200
Pb(TNR) • H_2O	–	–	260–310[38]	8[41]	0.45[41]	0.04–1[38]	15[41]
$Pb(N_3)_2$ (RD-1333)	–	–	320–350[38]	4[41]	≤ 0.1[41]	5–8[38]	37[41]

[a]Onset temperatures at a heating rate of 5 °C min^{-1}; [b]determined by 1 of 6 method; [c]endothermic peak, which indicates melting, phase transition, or loss of ligands; [d]exothermic peak, which indicates decomposition; [e]impact sensitivity (BAM drophammer test);[22] [f]friction sensitivity (BAM friction tester);[22] [g]electrostatic discharge sensitivity (OZM XSpark10);[39] [h]ball drop impact sensitivity (OZM BIT-132);[39,40] *endothermic signal followed by exothermic signal; n.d.: not determined.

The low sensitivity of complex **17**, especially compared to ECC **20** based on the same anion, is likely caused by grain size effects. While **17** (*FS* > 360 N, *IS* = 20 J) was investigated at a roughly determined grain size < 100 µm, the particle size distribution of **20** (*FS* = 192 N, *IS* = 3 J) was about 500–1000 µm, possibly making the sample more sensitive. Similar effects are assumed to be responsible for the difference within sensitivity data for compounds **19** (*IS* = 2 J, *FS* = 96 N) and **22b** (*IS* = 4 J, *FS* = 324 N). The difference in sensitivity between the two silver fulminate complexes is due to the content of fulminate in each complex. While in ECC **16a** two fulminate moieties occur on one ligand, in **16b** only one moiety is found per ligand. Therefore, complex **16a** is clearly more sensitive than **16b**.

Regarding the "UN Recommendations on the Transport of Dangerous Goods", except the ECCs **4**, **6**, **9**, and **17**, every compound must at least be classified as sensitive because of impact sensitivity measurements.[21] The complexes **5**, **7**, **8**, **11**, **13**, **14**, **16a**, and **19**–**21** even must be considered as very sensitive. The remaining compounds **4**, **9**, and **17** are classified as less sensitive. Taking into account the sensitivity toward friction, the zinc(II) chlorate complex **9** must be rated as very sensitive, with the compounds **7**, **13**, and **14** being extremely sensitive.

The synthesis of several complexes based on 1-NET has again extended the series of ECCs based on alkyl tetrazoles. This suggests a comparison of the complexes with each other, whereby the copper chlorate and perchlorate complexes probably appear to be the most suitable, since these, except for the chlorate complex based on 1-methyl-5*H*-tetrazole (MTZ), have the same structure. For this purpose, the data of different complexes known in the literature were compiled and plotted with the data of ECCs **8** and **13** from this work in the bar charts shown in Figure 12.[9,27,31]

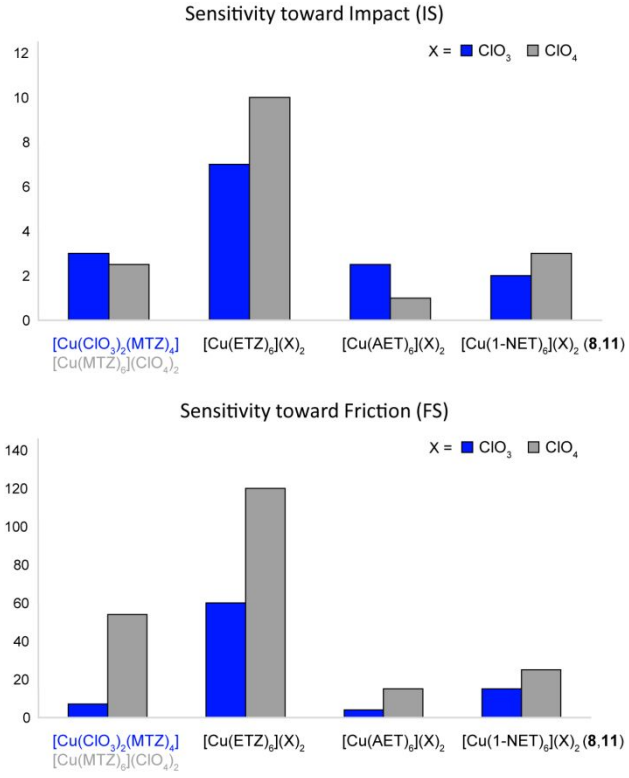

Figure 12. Bar charts displaying the impact sensitivity (top) and friction sensitivity (bottom) of selected copper(II) chlorate and perchlorate complexes based on various alkyl tetrazoles known in the literature.[9,27,31]

The charts generally indicate that a longer carbon chain without an additional energetic group leads to compounds being less sensitive. This is represented through the ECCs based on 1-ethyl-5*H*-tetrazole (ETZ). By adding an energetic group, like an azide (AET) or nitrate (NET), the effect gets less imminent, the resulting coordination compounds are even more sensitive than those based on 1-methyl-5*H*-tetrazole, having a shorter carbon chain. Regarding friction sensitivity another general trend can be observed, stating that chlorate complexes are always more sensitive than the ones based on perchlorate. When it comes to impact sensitivity, this tendency is less clear. It must be noted that the different structure of the methyl tetrazole chlorate complex might influence these findings. Comparing the complexes based on NET and AET shows that with the exception of $[Cu(AET)_6](ClO_3)_2$ (IS = 2.5 J), the complexes based on 1-azidoethyl-5*H*-tetrazoel are more sensitive.

Because of the already mentioned problems regarding BAM standard impact measurements, in this work, also ball drop impact sensitivity (BDIS) measurements were performed. The device is said to deliver results closer to realistic conditions due to a combination of spin and impact onto the sample.[41] Earlier works of our group showed that there are coherences between friction and ball drop impact. This work generally supports this thesis, with compounds **7**, **8**, **9**, **14**, **15**, and **21** being tested sensitive during both measurement types. However, the chlorate and perchlorate complexes are less sensitive toward BDIS which is likely due to the compounds melting point, resulting in crystals absorbing a lot of the impact energy. Major exceptions also are the compounds **11**, **19b**, and **22c**, which were tested less sensitive than expected. A reason explaining this behaviour might again be the particle size distribution or crystal shape. A highspeed image of the moment of impact of the compounds **13** and **14** is displayed in Figure 13.

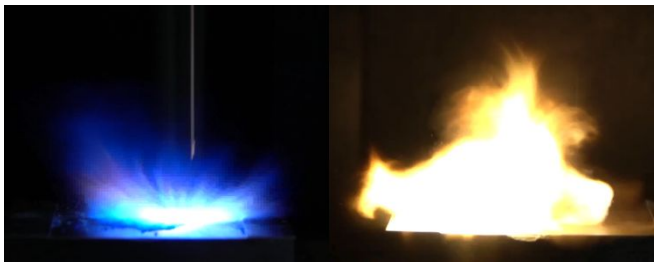

Figure 13. Moment of detonation during ball drop impact sensitivity measurements of the copper(II) perchlorate (**13**) and copper(II) azide complexes (**14**)

Hot Plate and Hot Needle Experiments

To get an insight into the compounds behaviour when exposed to fast heating, hot plate tests were performed for every ECC obtained elemental analysis pure. To run the test, the sample was placed on a copper plate and heated with a Bunsen burner until decomposition. An evaluation of the compounds' reaction when ignited under light confinement was made by applying hot needle tests. For this test the sample was fixed onto a copper plate by adhesive tape. Subsequently the compound was penetrated with a red glowing hot needle. Usually, a detonation in at least one of the tests is desired, as this outcome indicates a fast deflagration to detonation transition (DDT), which is an important property of a primary explosive. The DDT is said to allow conclusions to be drawn on how well a primary explosive is capable of igniting pentaerythritol tetranitrate (PETN). Since the substances are intended to rather serve as combustion catalysts than as primary explosives, deflagration or decomposition reactions are desired. The outcome of each test is displayed in Table 3, further high-speed images of the tests and details on the setup can be found in the General Information in the ESI†.

Deflagration reactions were observed for the majority of the investigated ECCs (Table 3). Only exceptions were the copper(II) azide complex **14** (Figure 14), and the silver(I) fulminate **16a**, which detonated during at least one of the experiments, together with compounds **9**, **17**, **19**, and **22b**, only decomposing during at least one of these experiments. Excluding ECCs **14** and **16a** this behaviour indicates a possible use as combustion catalyst. Based on these results, laser ignition experiments, and in case of **14**, **16a** and because of its strong deflagration also complex **7**, PETN initiation experiments are of interest. Compound **16b** showed a significant weaker reaction than ECC **16a** due to the lower fulminate content in the complex.

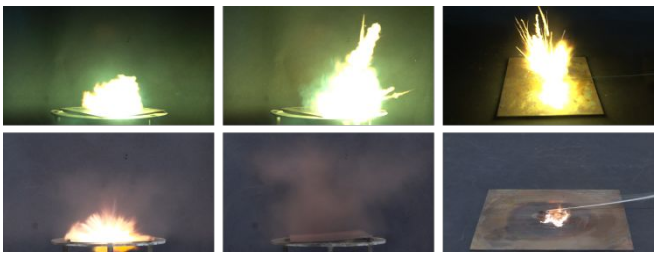

Figure 14. High-speed images of the results of the hot plate (left and middle) and hot needle tests (right picture) of the copper(II) dinitramide complex **7** (top) and the copper(II) azide coordination compound **14** (bottom).

PETN Initiation Experiments

The compounds which showed the most powerful behaviour during hot plate and hot needle tests have been found to be the dinitramide coordination compound **7**, the copper(II) azide complex **14**, and the silver fulminate ECC **16a.** These complexes showed either sharp deflagrations or even detonations during hot plate and hot needle tests. For their potential use as lead-free primary explosives, the compounds were tested towards their capability of initiating PETN. Therefore, 200 mg of the booster explosive was loaded into a copper shell and 50 mg of the test substance was filled on top (Figure 15, left). More details on the test setup can be found in the General Methods of the ESI.† A positive DDT from the primary explosive towards PETN is indicated by a hole in the copper witness plate and fragmentation of the shell. As illustrated in Figure 15 on the right, compound **14** successfully initiate PETN. In case of compounds **7**, and **16a** only negative results were obtained.

Table 3. Results of hot plate and hot needle experiments.[a]

Compound	No.	HP	HN	PETN	Laser Energy, E (mJ)[b]		
				Initiation	1.7	25.5	51.0
$[Cu(1\text{-}NET)_3(NO_3)_2]$	**6**	defl.	defl.	–	dec.	defl.	–
$[Cu(DN)_2(1\text{-}NET)_2]$	**7**	defl.	defl.	negative	det.	det.	–
$[Cu(1\text{-}NET)_6](ClO_3)_2$	**8**	defl.	defl.	–	–	dec.	–
$[Zn(1\text{-}NET)_6](ClO_3)_2$	**9**	defl.	dec.	–	–	–	–
$[Cu(1\text{-}NET)_6](ClO_4)_2$	**11**	defl.	defl.	–	–	dec.	–
$[Cu(2\text{-}NET)_6](ClO_4)_2$	**13**	defl.	defl.	–	–	dec.	–
$[Cu(N_3)_2(1\text{-}NET)]$	**14**	det.	det.	positive	–	det.	–
$[Ag_2(CNO)_2(1\text{-}NET)]$	**16a**	det.	defl.	negative	–	–	–
[Ag(CNO)(1-NET)]	**16b**	det.	dec.	–	–	–	–
$[Cu(1\text{-}NET)_2(PA)_2]$	**17**	defl.	dec.	–	–	comb.	comb.
$[Cu(1\text{-}NET)_2(TNR)]$	**18a**	defl.	defl.	–	–	comb.	comb.
$[Cu(H_2TNR)_2(1\text{-}NET)_4]$	**18c**	defl.	defl.	–	–	dec.	dec.
$[Cu(H_2TNPG)_2(1\text{-}NET)_4]$	**19**	defl.	dec.	–	–	comb.	comb.
$[Cu(2\text{-}NET)_2(PA)_2]$	**20**	defl.	defl.	–	–	dec.	dec.
$[Cu(2\text{-}NET)_2(TNR)]$	**21**	defl.	defl.	–	–	comb.	comb.
$[Cu(HTNPG)(2\text{-}NET)_2]$	**22a**	defl.	defl.	–		comb.	comb.
$[Cu(H_2TNPG)_2(2\text{-}NET)_4]$	**22b**	defl.	dec.	–	dec.	dec.	dec.
$[Cu(H_2TNPG)_2(2\text{-}NET)_4]$ • 2 2-NET	**22c**	defl.	defl.	–	det.	comb.	dec.

[a]–: not tested, comb.: combustion, dec.: decomposition, defl. Deflagration, det.: detonation; [b]Operating parameters: current I = 7 A; voltage U = 4 V; theoretical maximal output power P_{max} = 45 W; theoretical energy E_{max} = 1.7–51.0 mJ; wavelength λ = 915 nm; pulse length τ = 1–30 ms.

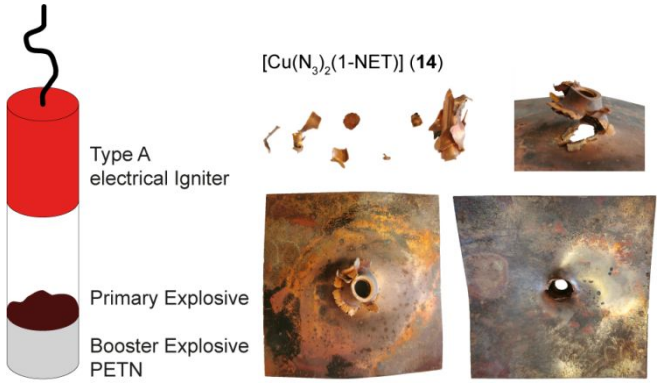

Figure 15. Left: Initiation test setup without copper witness plate. Right: Result of the initiation experiment of compound **14** toward PETN.

Laser Ignition Experiments

Especially in the field of primary explosives, the safe handling of materials is still severely limited since mechanical action is in many cases necessary for ignition.[1] For example, the pyrotechnic charges used in the percussion caps are ignited by frictional force generated by impact with the anvil. Therefore, the used energetic materials need to possess high sensitivities toward external stimuli like impact and friction. The sensitivity data of the most common primary explosives lead azide and lead styphnate monohydrate are displayed in Table 2. The sensitivity not only affects a safe preparation of the energetic materials, but it also makes processing and distribution more difficult.

However, new ways of ignition, which do not require mechanical stimuli, enable the use of less sensitive materials. One method that has received great attention in recent years is ignition through laser irradiation.[27,42,43] In order to make use of this new technique, every elemental analysis pure ECC prepared in this work were tested for their ignitability by laser. Since only coloured compounds are known to react during these experiments, testing of the zinc and silver complexes **9**, and **16** was waived. The outcome of each test and the respective energy used for ignition are displayed in Table 3. Further information on the test setup and procedure can be found in the General Information in the ESI†.

Interestingly not every of the compounds investigated, showed positive results during laser experiments. A decomposition (Table 3) indicates that no output was observed in the laser setup during laser irradiation. An inspection of the primer cap only showed changes of colour within the sample. A combustion (Figure 16, bottom right) was observed for most of the complexes based on trinitrophenolate anions. This is likely caused by the compounds' higher carbon content, resulting in lower energetic compounds. Detonations were observed for compounds **7** and **14**, which was expected with respect to the corresponding hot plate and hot needle tests (Figure 16, top right & bottom left). However, the results of complexes **8**, **11**, and **13** were surprising in terms of outcome. In previous experiments, chlorate, and perchlorate complexes proved to exhibit the strongest performance.[27,28,31] In this case only a slight decomposition within the primer cap was observed after the irradiation. This reinforces the theory that thermal ignition may be the reason for initiation and that the substances' low melting point may be a hindrance to this. Furthermore, pressing the substance into the caps also showed melting because of the force applied during compressing. Therefore, these substances are likely to find application as laser-ignitable energetic components only as a component of a mixture, and not as a neat substance.

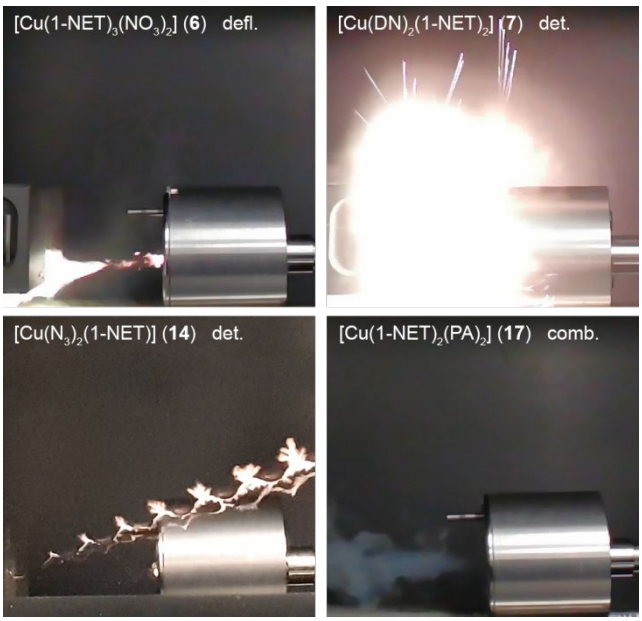

Figure 16. Single pictures of a high-speed movie of the reaction of the ECCs **6**, **7**, **14**, and **17** during laser ignition experiments at an energy of 25.5 mJ.

Conclusions

A one pot synthesis for 1-hydroxyethyl-5*H*-tetrazole was established in good overall yields by taking advantage of acetyl protection. A mixture of the 1- and 2-hydroxyethyl isomers was prepared by alkylation and after nitration with 100% nitric acid the mixture was separated by chromatographic methods. Both compounds 1-NET (1-nitratoethyl-5*H*-tetrazole) and 2-NET (2-nitratoethyl-5*H*-tetrazole), further used as ligands, were investigated by single crystal XRD and various NMR techniques, including ^{1}H, ^{13}C, ^{14}N, and ^{1}H ^{15}N HMBC. 2-NET was additionally investigated through ^{15}N NMR to clarify the atom assignment in the HMBC spectrum. BAM sensitivity measurements showed equal values for the friction sensitivity, however much higher impact sensitivities for the 2-isomer were observed. Molecular interactions were investigated to shed light on the sensitivity data. On the basis of Hirshfeld analysis, structural elements were investigated concluding that the rigid structure of 2-NET is likely to cause the increased sensitivity. The tetrazole derivatives were subsequently used for the preparation of 22 different metal (Mn, Cu, Zn, and Ag) complexes. Only acetonitrile and water were used as green solvents, with both the ligands and the resulting ECCs exhibiting a desirable poor solubility in water. Of these, with the exception of compound **13**, each was investigated using low temperature single crystal X-ray diffraction. Thus, 18 of these complexes were obtained elemental analysis pure and subsequently characterized with respect to their sensitivity toward impact, friction, ball drop impact, and electrostatic discharge. Especially the nitrate complex **6** (196 °C) and the trinitrophenolate based complexes **17** (197 °C) and **18a** (195°C) showed very good thermal stabilities, which are outstanding especially for organic nitrates. The improved oxygen balance due to this functional group, as well as the deflagration reactions of the compounds during hot plate and hot needle tests, reveal that these compounds can be considered as burn rate catalysts like basic copper nitrate (BCN). However, due to their energetic properties, they simultaneously improve the performance of the mixture. The laser ignition experiments showed that non-classical routes of initiation are also possible for the majority of these additives. Furthermore, these experiments indicate that the dinitramide complex **7** and azide complex **14** in particular are promising candidates as substitutes for BNCP. Because of a positive PETN initiation test, the latter compound is also interesting as a substitute for lead azide or lead styphnate.

Author Contributions

The manuscript was written through contributions of all authors. All authors have given approval to the final version of the manuscript.

Conflicts of Interest

There are no conflicts to declare.

Acknowledgements

The financial support of this work by the Ludwig-Maximilian University (LMU), the Office of Naval Research (ONR), under grant no. ONR N00014-19-1-2078, and the Strategic Environmental Research and Development Program (SERDP) under contract no. W912HQ19C0033 are gratefully acknowledged. Furthermore, the authors would like to thank Professor Dr. Konstantin Karaghiosoff for the measuring the ^{1}H-^{15}N NMR spectra, as well as Dr. Burkhard Krumm for the measurement of the ^{15}N NMR spectrum.

Notes and References

1 T. M. Klapötke, *High Energy Materials*, De Gruyter, Berlin, Boston, 5th edn., 2019.
2 A) D. Kumar, G. H. Imler, D. A. Parrish and J. M. Shreeve, *J. Mater. Chem. A*, 2017,**5**, 10437–10441; b) Y. Tang, K. Li, A. K. Chinnam, R. J. Staples and J. M. Shreeve, *Dalton Trans.*, 2021,**50**, 2143–2148; c) L. M. Barton, J. T. Edwards, E. C. Johnson, E. J. Bukowski, R. C. Sausa, E. F. C. Byrd, J. A. Orlicki, J. J. Sabatini and P. S. Baran, *J. Am. Chem. Soc.,* 2019, **141**, 12531–12535; d) J. Ma, H. Yang, J. Tang, G. Zhang, Z. Yi, S. Zhu and G. Cheng, *Dalton Trans.* 2020, **49**, 4675–4679; e) N. Lease, L. M. Kay , G. W. Brown, D. E. Chavez, D. Robbins, E. F. C. Byrd, G. H. Imler, D. A. Parrish and V. W. Manner, *J. Org. Chem.* 2020, **85**, 4619–4626.
3 M. A. S. Laidlaw, G. Filippelli, H. Mielke, B. Gulson and A. S. Ball, *Environ. Health* 2017, **16**, 34.
4 a) Candidate List of substances of very high concern for Authorisation, https://echa.europa.eu/de, (accessed May 2021); b) D. C. Dorman, S. H. Benoff, E. C. Bishop, M. L. Bleecker, L. M. Brosseau, R. H. Goldman, J. H. Graziano, S. A. Milz, S. K. Park and M. A. Roberts, *National Research Council Report: Potential Health Risks to DOD Firing-Range Personnel from Recurrent Lead Expo-sure*, National Academies Press, Washington, DC, USA, 2012.

5 T. Brinck, *Green Energetic Materials*; John Wiley & Sons Ltd., New York, 1st edn., 2014.
6 a) M. L. Gettings, M. T. Thoenen, E. F. C. Byrd, J. J. Sabatini, M. Zeller and D. G. Piercey, *Chem. Eur. J.* 2020, **26**, 14530–14535; b) N. Fischer, D. Fischer, T. M. Klapötke, D. G. Piercey and J. Stierstorfer, *J. Mater. Chem.* 2012, **22**, 20418–20422; c) S. Manzoor, Q. Tariq, X. Yin and J. Zhang, *Def. Technol.* 2021, in press; d) R. Meyer, J. Köhler and A. Homburg, *Explosives*, Wiley-VCH, Weinheim, 7th edn., 2016.
7 J. Roh, K. Vávrová and A. Hrabálek, *Eur. J. Org. Chem.* 2012, **2012**, 6101–6118.
8 P. N. Gaponik and V. P. Karavai, *Chem. Heterocycl. Compd*. 1985, **21**, 1172–1174.
9 a) P. N. Gaponik, V. P. Karavai and Yu. V. Grigor'ev, *Chem. Heterocycl. Compd*. 1985, **21**, 1255–1258; b) M. H. H. Wurzenberger, M. S. Gruhne, M. Lommel, N. Szimhardt, T. M. Klapötke and J. Stierstorfer, *Chem. Asian J.* 2019, **14**, 2018–2028.
10 T. M. Klapötke, B. Krumm, T. Reith, and C. C. Unger, *J. Org. Chem.* 2018, **83**, 10505−10509.
11 a) M. S. Ghasemzadeh and B. Akhlaghinia, *ChemistrySelect* 2020, **5**, 6440–6452; b) A. F. Stassen, M. Grunert, E. Dova, H. Schenk, G. Wiesinger, M. Müller, P. Weinberger, W. Linert, J. G. Haasnoot and J. Reedijk, *Eur. J. Inorg. Chem.* 2003, **2003**, 2273–2282.
12 a) K. A. McDonald, S. Seth and A. J. Matzger, *Cryst. Growth Des.* 2015, **15**, 5963–5972; b) Q. Zhang and J. M. Shreeve, *Angew. Chem. Int. Ed.* 2014, **53**, 2540–2542; c) H. Gao, Q. Zhang and J.M. Shreeve, *J. Mater. Chem. A*, 2020, **8**, 4193–4216.
13 R. N. Roberts and R. H. Dinegar, *J. Phys. Chem.* 1958, **62**, 1009–1011.
14 N. Fischer, T. M. Klapötke, J. Stierstorfer and C. Wiedemann, *Polyhedron* 2011, **30**, 2374–2386.
15 J. Stierstorfer, K. R. Tarantik and T. M. Klapötke, *Chem. Eur. J.* 2009, **15**, 5775–5792.
16 L. Zeisel, N. Szimhardt, M. H. H. Wurzenberger, T. M. Klapötke and J. Stierstorfer, *New J. Chem.* 2019, **43**, 609–616.
17 T. M. Klapötke, J. Stierstorfer and B. Weber, *Inorg. Chim. Acta* 2009, **362**, 2311–2320.
18 K. Shiota, H. Matsunaga and A. Miyake, *J. Therm. Anal. Calorim.* 2015, **121**, 281–286.
19 a) D. E. Bayes, *Eu. Pat.*, EP011736 8A1, 1982; b) T. M. Klapötke and S. M. Sproll, *Eur. J. Org. Chem.* 2010, **2010**, 1169–1175.
20 W. G. Finnegan and R. A. Henry, *J. Org. Chem*. 1959, **24**, 1565–1567.
21 UN Model Regulation: Recommendations on the Transport of Dangerous Goods – Manual of Tests and Criteria, section 13.4.2.3.3, 2015.
22 a) BAM, http://www.bam.de, (accessed April May); b) NATO standardization agreement (STANAG) on explosives, impact sensitivity tests, no. 4489, 1st edn., Sept. 17th, 1999; c) WI–WEB–Standardarbeitsanweisung 4–5.1.02, Ermittlung der Explosionsgefährlichkeit, hier der Schlagempfindlichkeit mit dem Fallhammer, Nov. 8th, 2002; d) NATO standardization agreement (STANAG) on explosive, friction sensitivity tests, no. 4487, 1st edn., Aug. 22nd, 2002; e) WIWEB-Standardarbeitsanweisung 4-5.1.03, Ermittlung der Explosionsgefährlichkeit oder der Reibeempfindlichkeit mit dem Reibeapparat, Nov. 8th, 2002.
23 a) M. J. Turner, J. J. McKinnon, S. K. Wolff, D. J. Grimwood, P. R. Spackman, D. Jayatilaka and M. A. Spackman, CrystalExplorer17, University of Western Australia, 2017; b) M. A. Spackman and D. Jayatilaka, *CrystEngComm* 2009, **11**, 19–32.
24 a) C. Zhang, X. Xue, Y. Cao, Y. Zhou, H. Li, J. Zhou and T. Gao, *CrystEngComm*. 2013, **15**, 6837–6844; b) Y. Ma, A. Zhang, X. Xue, D. Jiang, Y. Zhu and C. Zhang, *Cryst. Growth Des*. 2014, **14**, 6101−6114.
25 J. G. Reynolds, P. C. Hsu, G. A. Hust, S. A. Strout and H. K. Springer, *Propellants Explos. Pyrotech*. 2017, **42**, 1303–1308.
26 M. Sućeska, EXPLO5 Version 6.05 User's Guide. Zagreb, Croatia: OZM; 2018.
27 N. Szimhardt, M. H. H. Wurzenberger, A. Beringer, L. J. Daumann and J. Stierstorfer, *J. Mater. Chem*. *A*, 2017, **5**, 23753–23765
28 N. Szimhardt, M. H. H. Wurzenberger, L. Zeisel, M. S. Gruhne, M. Lommel and J. Stierstorfer, *J. Mater. Chem. A* 2018, **6**, 16257–16272.
29 M. H. H. Wurzenberger, B. R. G. Bissinger, M. Lommel, M. S. Gruhne, N. Szimhardt and J. Stierstorfer, *New J. Chem*. 2019, **43**, 18193–18202.
30 M. S. Gruhne, M. H. H. Wurzenberger, M. Lommel and J. Stierstorfer, *Chem. Eur. J.* 2021, in press.
31 M. H. H. Wurzenberger, N. Szimhardt and J. Stierstorfer, *J. Am. Chem. Soc*. 2018, **140**, 3206–3209.
32 M. H. H. Wurzenberger, M. Lommel, M. S. Gruhne, N. Szimhardt and J. Stierstorfer, *Angew. Chem. Int. Ed*. 2020, **59**, 12367–12370.
33 M. H. H. Wurzenberger, M. S. Gruhne, M. Lommel, V. Braun, N. Szimhardt and J. Stierstorfer, *Inorg. Chem*. 2020, **59**, 17875–17879.
34 Crystallographic data for the structures have been deposited with the Cambridge Crystallographic Data Centre. Copies of the data can be obtained free of charge on application to The Director, CCDC, 12 Union Road, Cambridge CB2 1EZ, UK (Fax: int.code_(1223)336-033; e-mail for inquiry: fileserv@ccdc.cam.ac.uk; e-mail for deposition: (deposit@ccdc.cam.ac.uk).
35 T. Lenz, T. M. Klapötke, M. Mühlemann and J. Stierstorfer, *Propellants Explos. Pyrotech.* 2021, **46**, 723–731.
36 T. Ohtake, S. Date, K. Ikeda and Y. Shiraishi, *Sci. Tech. Energetic Materials* 2015, **76**, 39–41.
37 a) L. M. Foroughi, R. A. Wiscons, D. R. Du Bois and A. J. Matzger, *Chem. Commun*. 2020, **56**, 2111–2114; b) M. K. Bellas and A. J. Matzger, *Angew. Chem. Int. Ed*. 2019, **58**, 17185–17188.
38 T. M. Klapötke, *Energetic Materials Encyclopedia*, De Gruyter, Berlin, Boston, 2nd edn., 2021.
39 OZM Research, http://www.ozm.cz/en, (accessed May 2021).
40 Military Standard 1751A (MIL-STD-1751A): safety and performance tests for qualification of explosives (high explosives, propellants and pyrotechnics), method 1016, Dec. 11st, 2001.
41 M. S. Gruhne, M. Lommel. M. H. H. Wurzenberger, N. Szimhardt, T. M. Klapötke and J. Stierstorfer, *Propellants Explos. Pyrotech*. 2020, **45**, 147–153.
42 T. W. Myers, J. A. Bjorgaard, K. E. Brown, D. E. Chavez, S. K. Hanson, R. J. Scharff, S. Tretiak and J. M. Veauthier, J. *Am. Chem. Soc.* 2016, **138**, 4685–4692.
43 M. A. Ilyushin, A. A. Kotomin and S. A. Dushenok, *Russ. J. Phys. Chem B* 2019, **13**, 119–138.